Functional analyses of differentially expressed isoforms of the Arabidopsis inositol phosphorylceramide synthase

J. G. Mina[1,2#], Y. Okada[3#], N. K. Wansadhipathi-Kannangara[1,2], S. Pratt[1,2], H. Shams-Eldin[4], R. T. Schwarz[4,5], P. G. Steel[1], T. Fawcett[3*] and P. W. Denny[1,2*]

[1]Centre for Bioactive Chemistry, Department of Chemistry and School of Biological and Biomedical Sciences, Durham University, U.K.; [2]School of Medicine and Health, Durham University, Queen's Campus, Stockton-on-Tees, U.K.; [3]School of Biological and Biomedical Sciences, Durham University, U.K.; [4]Institute for Virology, Medical Center of Hygiene & Medical Microbiology, Philipps-University Marburg, Germany; [5]Unité de Glycobiologie Structurale et Fonctionnelle, Université des Sciences et Technologies de Lille, France.

# These authors contributed equally to this work.

* Corresponding authors : p.w.denny@durham.ac.uk and tony.fawcett@durham.ac.uk

Abbreviations: AbA – aureobasidin A; BSA – bovine serum albumin; Cer – ceramide; IPC – inositol phosphorylceramide; NDB C_6-ceramide – 6-((N-(7-nitrobenz-2-oxa-1,3-diazol-4-yl)amino) hexanoyl)sphingosine; PI – phosphatidylinositol; SD – synthetic minimal media with glucose; SGR – synthetic minimal media with galactose; SM – sphingomyelin

Abstract

Sphingolipids are key components of eukaryotic plasma membranes that are involved in many functions, including the formation signal transduction complexes. In addition, these lipid species and their catabolites function as secondary signalling molecules in, amongst other processes, apoptosis. The biosynthetic pathway for the formation of sphingolipid is largely conserved. However, unlike mammalian cells, fungi, protozoa and plants synthesize inositol phosphorylceramide (IPC) as their primary phosphosphingolipid. This key step involves the transfer of the phosphorylinositol group from phosphatidylinositol (PI) to phytoceramide, a process catalysed by IPC synthase in plants and fungi. This enzyme activity is at least partly encoded by the *AUR1* gene in the fungi, and recently the distantly related functional orthologue of this gene has been identified in the model plant Arabidopsis. Here we functionally analysed all three predicted Arabidopsis IPC synthases, confirming them as aureobasidin A resistant AUR1p orthologues. Expression profiling revealed that the genes encoding these orthologues are differentially expressed in various tissue types isolated from Arabidopsis.

Key words: Arabidopsis, AUR1, expression, inositol phosphorylceramide, IPC synthase, sphingolipids

Introduction

The diverse, amphipathic sphingolipids consist of a long chain base backbone with long-chain fatty acid and polar alcohol attachments. These lipid species are ubiquitous membrane components of eukaryotic cells, as well as being found in some prokaryotic organisms and viruses (Smith and Merrill 2002). Studies in mammals and yeast have shown that they are important structural components of membranes and also serve as bioactive molecules involved in cell signalling and regulation (Dickson, et al. 2006; Fernandis and Wenk 2007; Hanada, et al. 1992). The unmodified sphingolipid, ceramide, is an intermediate in complex sphingolipid biosynthesis in the Golgi apparatus. These complex species ultimately concentrate in the outer leaflet of the plasma membrane where, with sterols, they form lipid raft microdomains (Futerman and Hannun 2004). Rafts have been proposed to be central to a multitude of cellular processes, from the polarized trafficking of lipid-modified proteins (Brown and London 1998) to the formation of signal transduction complexes (Magee, et al. 2002; Pierce 2002). Furthermore, sphingolipid metabolites such as ceramide and phosphorylated sphingosine (sphingosine-1-phosphate), are central to intracellular signal transduction processes that regulate cell growth, differentiation and apoptosis (programmed cell death – PCD; Futerman and Hannun 2004).

The biosynthesis of sphingolipids shows commonality between mammals, fungi and plants up to the formation of ceramide (phytoceramide in plants and fungi), but the predominant complex phosphosphingolipid species subsequently synthesized differs. Mammals produce sphingomyelin (SM; a ceramide unit with a phosphorylcholine moiety), whereas fungi and plants synthesize inositol phosphorylceramide (IPC) by the transfer of the phosphorylinositol group from phosphatidylinositol (PI) to phytoceramide, a reaction catalysed by IPC synthase. This enzyme was shown to be at least partly encoded by the *AUR1* gene in yeast and other fungi (Nagiec, et al. 1997), and recently an accessory protein involved in IPC synthase activity (KEI1p) in these organisms has been identified (Sato, et al. 2009). However, the plant enzyme remained unidentified although the activity had been

measured in bean microsomes (Bromley, et al. 2003). Then, during a screen for factors involved in PCD defence mechanisms, an *AUR1* functional orthologue was identified in Arabidopsis. However, the encoded protein demonstrated little homology to the yeast AUR1p, having most similarity to the more recently identified animal sphingomyelin synthases (Wang, et al. 2008). This lack of similarity to the long known fungal enzyme (Nagiec, et al. 1997) lay behind the previously fruitless search for the plant orthologue (Dunn, et al. 2004).

Here we demonstrate that all three orthologues identifiable in the Arabidopsis genome database represent aureobasidin A resistant functional orthologues and that, through phylogenetic analyses, these represent a new group of sphingolipid synthases within the wider enzyme family. Furthermore, we show the expression profile of all three isoforms in the tissues of Arabidopsis. This demonstrated that there is differential expression of IPC synthase, an enzyme central to the synthesis of plasma membrane sphingolipids (Dunn et al. 2004) and a regulator of PCD (Wang, et al. 2008) in this plant species.

Materials and Methods

Complementation of auxotrophic AUR1 mutant yeast with AtIPCS1-3

Arabidopsis IPC synthase 1, 2 and 3 (AtIPCS1 - At3g54020.1, AtIPCS2 - At2g37940.1 and AtIPCS3 - At2g29525.1) were amplified from Arabidopsis cDNA using primers

5' AtIPCS1 EcoRI gaattcATGACGCTTTATATTCGCCGCG and 3' AtIPCS1 SalI gtcgacGAGCAGAGATCTCATGTGCC;

5' AtIPCS2 EcoRI gaattcATGACACTTTATATTCGTCGTG and 3' AtIPCS2 SalI gtcgacTCACGCGCCATTCATTGTG;

5' AtIPCS3 EcoRI gaattcATGCCGGTTTACGTTGATCGCG and 3' AtIPCS3 SalI gtcgacTCAATGATCATCTGCTACATTG.

The products were subsequently cloned into the yeast vector pRS426MET25, creating pRS426 AtIPCS1-3. In the YPH499–HIS–GAL–AUR1 *S. cerevisiae* strain expression of the essential *AUR1* gene (Nagiec, et al. 1997) is under the control of the *GAL1* promoter and is repressed in the presence of glucose (Denny, et al. 2006). YPH499–HIS–GAL–AUR1 was transformed with pRS426 AtIPCS1-3 and pRS426 AUR1 and functionally complemented transformants selected on non-permissive SD medium containing necessary nutritional supplements (Denny, et al. 2006).

Diffusion assay of complemented auxotrophic AUR1 mutant yeast

YPH499–HIS–GAL–AUR1 pRS246 AtIPCS1-3 and YPH499–HIS–GAL–AUR1 pRS246 AUR1 were assayed for susceptibility to aureobasidin A (Takara) and myriocin (Sigma) as previously described (Nagiec, et al. 2003). Briefly, $2.4x10^7$ logarithmically dividing cells were embedded in 15 ml of YPD-agarose (1% yeast extract, 2% peptone, 2% dextrose, 0.8% agarose) on 100 mm^2 square Petri dishes (Sarstedt). Inhibitors were applied in Me_2SO at the concentrations described below and the dishes incubated at 30°C.

Microsomal assay of AtIPCS

For *in vitro* assay microsomal membranes were prepared from YPH499–HIS–GAL–AUR1 pRS246 AtIPCS1-3 and YPH499–HIS–GAL–AUR1 pRS246 AUR1 and assayed as described (Mina, et al. 2009)**.** In brief, assays were performed in 50µl of 100mM Tris HCl pH 7.4, 10mM EDTA and 6mg/ml defatted BSA, with or without 1mM PI (soybean, Avanti Polar Lipids; predominant species C16:0-C18:2) and 5µM aureobsidin A, and with 2 µl of microsomes (10 mg/ml protein) and 2µl of 5mM NBD C_6-Ceramide (Molecular Probes) in DMSO. After incubation at 30°C for 60 min the reaction was stopped by the addition of 150µl of chloroform/methanol/water (10:10:3 v/v/v) and the lipid fraction isolated by phase separation. This process facilitated reproducible quantitative analyses of IPC formation. Following equilibriation (Synergy HT, Bio-tek) samples were analysed by high performance thin-layer chromatography (Denny, et al. 2001; Ralton and McConville 1998), imaged using a FLA3000 scanner (Fuji) and quantified using the Aida V3.11 software package.

Plant growth and harvesting of material

Arabidopsis thaliana (Col-0) plants were grown under long-day conditions (16 h day/8 h night) and the following tissues were harvested at specific development stages (Boyes, et al. 2001). Rosette leaves were collected at stage 3.90, cauline leaves and stem were collected at stage 5.10, roots and flowers were collected at stage 6.50, siliques were collected at stage 8.00.

RNA Isolation and RT

Plant tissue was harvested and immediately frozen in liquid nitrogen. Total RNA was isolated using an RNeasy Plant Mini Kit (Qiagen), including DNAse I digestion, according to the manufacturers instructions.

RNA integrity was tested by electrophoresis on 1% agarose gels and was quantified by measuring the absorbance at 260 nm. The $A_{260\ nm}/A_{280\ nm}$ ratios of purified RNA samples were in the range of 2.0 to 2.1 and were determined to be free of genomic DNA by the absence of larger, intron containing, PCR

products.

RT reactions were carried out on 1.0µg of total plant RNA using Superscript III reverse transcriptase (Invitrogen) and oligo dT primer according to the manufacturers instructions.

Real-Time qRT-PCR conditions and analysis

Steady-state levels of RNA for each AtIPCS gene in plant material were analysed using SYBR green to monitor DNA synthesis with a Rotor-Gene RG-3000 (Corbett Research) instrument. Amplification was achieved with the following gene-specific primers; AtIPCS1-forward 5'-AGCCTCTTGATTATTGCGTC-3' and AtIPCS1-reverse 5'-AACAACGGCATTGCTCCCT-3' to give a 145 bp product; AtIPCS2-forward 5'-AGCCTCTTGATCATTGCCTC-3' and AtIPCS2-reverse 5'-GACTGCTGTGTTGCTCCCA-3' to produce a 145 bp product; AtIPCS3-forward 5'-TGGCTTATGGCAGTAATACAG-3' and AtIPCS3-reverse 5'-GCCAGAAATGGCAGAACGTTCT-3' to produce a 141 bp product. To determine the highest specificity and sensitivity qPCR profile for each AtIPCS transcript, titration experiments were performed over a range of $MgCl_2$ concentrations (1.5 to 5 mM) and primer concentrations from (0.1 to 0.5 μM). Concentrations were considered optimal at the lowest C_T value that reproducibly gave an amplicon of the correct size in the absence of primer dimers. Based on results of these optimization experiments, qPCR assays for the AtIPCS1 transcript contained 3 mM $MgCl_2$ and 0.5 μM of each primer; the AtIPCS2 transcript 3 mM $MgCl_2$ and 0.4 μM of each primer; and the AtIPCS3 transcript 4 mM $MgCl_2$, 0.4 μM of the forward and 0.5 μM of the reverse primer. The reactions (total volume 20 μl) also contained 2 μl of 10X PCR buffer, 10 pg of cDNA, 200 μM dNTPs, SYBR Green I dye and 2 Units of Taq polymerase. Assays were carried out using the following conditions: 1 cycle of 10 min of 95^{o}C, followed by 30 cycles of 10 sec of 95 ^{o}C, 15 at 52 ^{o}C and 20 sec of 72 ^{o}C. Amplicon dissociation curves were recorded at the end of the PCR cycles. External standard curves were constructed using the three AtIPCS cDNAs and relevant gene-specific primer pairs and used to determine the number of transcripts for each gene.

Results

AtIPCS1-3 complement an *AUR1* auxotrophic mutant yeast and confer aureobasidin A resistance

Interrogation of the Arabidopsis genome database with the predicted protein sequence of the protozoan IPC synthase from *Leishmania major* (*Lm*IPCS) (Denny, et al. 2006) identified opening reading frames encoding three highly related sequence orthologues – Arabidopsis IPC synthase 1 (AtIPCS1 - At3g54020.1), AtIPCS2 (At2g37940.1) and AtIPCS3 (At2g29525.1) – demonstrating 26%, 29% and 31% identity to the protozoan protein. Subsequently, AtIPCS2 has been isolated, characterised and designated ERH1 (Wang, et al. 2008). The open reading frames of AtIPCS1-3, when cloned into an URA3 selectable expression vector to create pRS426 AtIPCS1-3, restored the growth of the *AUR1* auxotrophic mutant YPH499-HIS-GAL-AUR1, as did the ectopic expression of *S. cerevisiae* AUR1p (AUR1) (figure 1A). These data indicated that AtIPCS1, 2 and 3 are functional orthologues of fungal AUR1p, a protein that forms at least part of an IPC synthase (Nagiec, et al. 1997).

By diffusion assay (Nagiec, et al. 1997; Nagiec, et al. 2003) the efficacy of two different classes of inhibitor were assayed against YPH499-HIS-GAL-AUR1 pRS426 AtIPCS1, 2 and 3. The transgenic yeast were resistant to aureobasidin A (AbA, a fungal IPC synthase inhibitor) at 100μM (figure 1B), a concentration shown to inhibit the growth of *Lm*IPCS complemented yeast (Denny, et al. 2006), but remained sensitive to myriocin (which inhibits the first step in sphingolipid biosynthesis - serine palmitoyltransferase, SPT). Indeed, yeast complemented with the plant enzymes appeared to be more sensitive to the SPT inhibitor than the AUR1 control, a similar observation had previously been made with regard to the *Lm*IPCS complemented yeast (Denny, et al. 2006). The *in vitro* assay for AtIPCS1-3 described below (figure 2A) confirmed that the Arabidopsis enzymes are AbA insensitive. In contrast, the IPCS activity from Golden butterwax bean extracts has been shown to be acutely

sensitive to this inhibitor (Bromley, et al. 2003). The reasons for this difference in AbA sensitivity are unclear and no data are currently available, for the bean sequence, to help elucidate this discrepancy.

AtIPCS1-3 are functional IPC synthases

In vitro assay of microsomes prepared from YPH499-HIS-GAL-AUR1 pRS426 AtIPCS1-3 demonstrated that the three plant enzymes are active IPC synthases (figure 2A). However, their turnover appeared low when compared to an *S. cerevisiae* AUR1 control. This was also noted by Wang et al (2008) and was unaffected by the use of NBD C_6-phytoceramide rather than C_6-ceramide as acceptor substrate. In support of the data shown above (figure 1B), AtIPCS1-3 activity was insensitive to the addition of AbA at a concentration (5 μM) that completely inhibited the yeast enzyme (figure 2A). Thereafter this inhibitor was applied to the reaction mix for assay of AtIPCS1-3 at 5 μM.

In the experiment (figure 2A) above the plant (and yeast) enzymes are assayed in the presence of exogenous soybean PI. To ascertain the effect of adding this exogenous donor substrate samples were assayed with and without PI in the reaction mix (figure 2B). All samples showed a similar level of activity in the absence of donor substrate but, surprisingly, only AtIPCS2 demonstrated any significant increase in turnover on the addition of PI. This indicated that the AtIPCS1 and 3 are unable to utilize substrate from this source effectively. Similar results were obtained utilizing bovine PI which has previously been demonstrated to be effectively utilized by the protozoan orthologues from both *L. major* and *Trypanosoma brucei* but not by *S. cerevisiae* AUR1p (Mina, et al. 2009). Despite this, these data confirm AtIPCS1-3 as functional orthologues of AUR1p, forming at least part of an IPC synthase.

The plant IPC synthases form a new class of sphingolipid synthase

The key motifs, D3 and D4, of the sphingolipid synthase family are conserved in the plant IPC synthases (Wang, et al. 2008). However, unlike their protozoan and mammalian counterparts they lack a D1 domain (Huitema, et al. 2004). In this they resemble the fungal IPC synthases and it may be hypothesized that D1 is involved in the binding of ceramide, a substrate for the protozoan and mammalian enzymes, whereas another unidentified region is involved in binding the phytoceramide substrate to the plant and fungal IPC synthases. Despite the conservation of some of these motifs the plant sequences are divergent with respect to primary sequence and so, until recently, remained cryptic within the genome databases (Wang, et al. 2008). This divergence was illustrated by phylogenetic analysis of predicted SM and IPC synthase sequences which demonstrated that the plant enzymes, the three orthologues identified in the *Oryza sativa* (rice) database are included, form a new clade of sphingolipid synthases (figure 3).

Expression profiling of AtIPCS1-3

Estimates of the relative abundance of transcripts can be made from their representation within the EST databases. For the three AtIPCS genes described a similar number of AtIPCS1 and AtIPCS3 transcripts are present, whilst the largest number is for AtIPCS2 (Table 1; data derived from TAIR BLAST version 2.2.8). However, these data do not give any information regarding the tissue location of the transcripts and are therefore of limited use when investigating the expression of gene families. Tissue-specific transcript abundance data can be obtained from multiple microarray experiments using Genevestigator (Grennan 2006). Only AtIPCS2 is represented on the Affymetrix arrays that are used to derive these data and this shows that the gene is expressed in cauline leaves, roots and rosette leaves at similar levels and these are approximately twice the expression levels seen in stems, flowers and siliques (Table 2).

Given the limitations of these data sets, in order to establish a complete expression profile for each AtIPCS isoform, real time quantitative RT-PCR was performed on RNA isolated from various Arabidopsis tissues (figure 4).

AtIPCS2 was the most highly expressed of the three isoforms in all tissues. In agreement with the Genevestigator data, the highest levels of AtIPCS2 transcript were seen in root, rosette leaves and cauline leaves and these were five to ten fold greater than the levels of transcripts in siliques, stems and flowers. The patterns of expression determined by these two methods are in general agreement but the relative levels differ, this may reflect differences in the plant material used in the each case. Genevestigator uses a large number of microarray experiments to generate data and is therefore robust, however the data represents plant material grown under different conditions and which may have been harvested at different times within a developmental stage. The quantitative RT-PCR data presented here is determined from plants grown and harvested under identical conditions and therefore represents transcript levels at defined developmental stages in these tissues.

AtIPCS1 transcripts are expressed at low levels in all tissues, ranging from 0.05% of AtIPCS2 levels in rosette leaves to 2.8% of AtIPCS2 levels in stems. While AtIPCS3 transcripts are also present in low levels in cauline leaves, rosette leaves, roots and stems (ranging from 0.02% to 0.67% of AtIPCS2 transcripts) they are present at similar levels to AtIPCS2 transcripts in stem (84 % of AtIPCS2 levels) and flower (74% of AtIPCS2 levels).

The data presented here adds to existing studies by providing tissue specific expression data for all the isoforms of AtIPCS which may indicate a specific role for AtIPCS3 in stems and flowers.

Discussion

The data presented describe the analyses of all three orthologues of the recently identified Arabidopsis IPC synthase (Wang, et al. 2008). They all represented functional orthologues of *S. cerevisiae* IPC synthase, AUR1p, and demonstrated activity in an *in vitro* assay. However, unlike the yeast activity the Arabidopsis enzyme is resistant to aureobasidin A, a non-competive inhibitor of the fungal IPC synthase with an unknown mechanism of action (Zhong, et al. 1999). Conversely, it has previously been shown that the IPCS activity in Golden butterwax bean extracts was acutely sensitive to this inhibitor (Bromley, et al. 2003). The reasons for this discrepancy are unclear, however it is notable that similarly profound differences in aureobasidin A sensitivity have been observed within the kinetoplastid parasite IPCS orthologues. Whilst the *L. major* enzyme is relatively refractory to the drug, the *T. brucei* sphingolipid synthase (TbSLS) is highly sensitive (Mina, et al. 2009). No reason for this can be deduced from the primary sequence data and it may be envisaged that this diversity is due to subtle differences in 3-dimensional enzyme structure.

In the *in vitro*, microsome-based assay all three Arabidopsis isoforms demonstrated IPC synthase turnover. However, although the presence of PI (from soybean or bovine sources) led to a significant increase in turnover with AtIPCS2, AtIPCS1 and 3 were refractory to the addition of this donor substrate. This indicated that PI from these sources was utilized inefficiently by these Arabidopsis isoforms. Similarly, it has been noted that mammalian PI is not efficiently utilized by the *S. cerevisiae* IPC synthase activity (Mina, et al. 2009). Notably, unlike the yeast phospholipids (Guan and Wenk 2006), plant and mammalian PIs exhibit varying degrees of polyunsaturation (Thompson and MacDonald 1975; Thompson and MacDonald 1976). It may be hypothesized this polyunstauration may confer structural constraints and make it less acceptable to the *S. cerevisiae* enzyme. However, the lack of reactivity of AtIPCS1 and with plant derived PI (soybean, C16:0-C18:2) is less easy to explain. It is possible that the endogenous yeast PI has a higher affinity for these isoforms and outcompetes the exogenous substrate.

Attempts to minimize the available quantity of endogenous PI to test this were made by detergent washing as previously (Mina, et al. 2009). However, this led to apparent inactivation of the enzymes. Alternatively, significant differences may exist in the substrate requirements of these Arabidopsis isoforms. Notably, AtIPCS1 transcript level is low in all plant tissue and AtIPCS3 in many, including siliques, perhaps reflecting the level of acceptable donor PI in seeds (such as soybeans, the source of PI in these experiments).

Despite these variances, all the plant IPC synthase orthologues identified share the motifs predicted to form the catalytic triad that promotes nucleophilic attack on lipid phosphate ester bonds which, in the case of IPC synthase, is thought to lead to the transfer of an inositol phosphate group from PI to the 1-hydroxyl group of (phyto)ceramide releasing diacylglycerol as a by-product (Huitema, et al. 2004; Neuwald 1997). Therefore it is likely that the eukaryotic sphingolipid synthases possess a common mechanism of action, indicating a single evolutionary origin. In contrast, the prokaryotic SM synthase lacks the catalytic triad (Luberto, et al. 2003) and is likely to have evolved independently. Phylogenetic analyses show the plant proteins forming a distinct clade, thereby defining a new class of eukaryotic sphingolipid synthases.

It has been demonstrated, by RNAi of the first enzyme in the biosynthetic pathway - serine palmitoyltransferase, that sphingolipid biosynthesis *per se* is essential for the viability of Arabidopsis (Chen, et al. 2006). Furthermore, recent work has suggested that the plant IPC synthase is pivotal in pathogen-resistance associated PCD. By analyses of leaf tissue from an ERH1 (AtIPCS2) insertion mutant Wang et al (2008) detected a significant increase in ceramide levels, an observation consistent with the fact that ceramide is a substrate for IPCS. Importantly, ceramide is a key regulator of PCD (Futerman and Hannun 2004) and the accumulation of this factor was co-incident with PCD at the site of powdery mildew infection in Arabidopsis (Wang, et al. 2008). This work is further supported by similar observations in accelerated-cell-death (*acd11* and *acd5*) mutants of Arabidopsis in which a sphingosine transfer protein (ACD11) or a ceramide kinase (ACD5) are affected (Brodersen, et al. 2002; Liang, et al. 2003). Given the prominence of

AtIPCS2 as a putative regular of PCD the differential expression levels of each of the three functional Arabidopsis orthologues may shed light on this key process in the whole plant.

Acknowledgements

This work was funded by Biotechnology and Biological Research Council (BB/D52396X/1) and Royal Society (2005/R1) grants to PWD and a British Council/Deutscher Akademischer Austausch Dienst Academic Research Collaboration Award to PWD and RTS. JGM and NKW are funded by the Overseas Research Student Award Scheme. JGM is also funded by the Wolfson Research Institute. This work was also supported in part by the Wolfson Research Institute Collaborative Small Grants Scheme and Deutsche Forschungsgemeinschaft, Bonn.

References

Boyes DC, Zayed AM, Ascenzi R, McCaskill AJ, Hoffman NE, Davis KR, Gorlach J (2001) Growth stage-based phenotypic analysis of arabidopsis: A model for high throughput functional genomics in plants. Plant Cell 13:1499-1510

Brodersen P, Petersen M, Pike HM, Olszak B, Skov S, Odum N, Jorgensen LB, Brown RE, Mundy J (2002) Knockout of Arabidopsis accelerated-cell-death11 encoding a sphingosine transfer protein causes activation of programmed cell death and defense. Genes Dev 16:490-502

Bromley PE, Li YNO, Murphy SM, Sumner CM, Lynch DV (2003) Complex sphingolipid synthesis in plants: characterization of inositolphosphorylceramide synthase activity in bean microsomes. Archives of Biochemistry and Biophysics 417:219-226

Brown DA, London E (1998) Functions of lipid rafts in biological membranes. Annu Rev Cell Dev Biol 14:111-136

Chen M, Han G, Dietrich CR, Dunn TM, Cahoon EB (2006) The essential nature of sphingolipids in plants as revealed by the functional identification and characterization of the Arabidopsis LCB1 subunit of serine palmitoyltransferase. Plant Cell 18:3576-3593

Denny PW, Field MC, Smith DF (2001) GPI-anchored proteins and glycoconjugates segregate into lipid rafts in Kinetoplastida. FEBS Lett 491:148-153

Denny PW, Shams-Eldin H, Price HP, Smith DF, Schwarz RT (2006) The protozoan inositol phosphorylceramide synthase: A novel drug target which defines a new class of sphingolipid synthase J Biol Chem 281:28200-28209

Dickson RC, Sumanasekera C, Lester RL (2006) Functions and metabolism of sphingolipids in Saccharomyces cerevisiae. Prog Lipid Res 45:447-465

Fernandis AZ, Wenk MR (2007) Membrane lipids as signaling molecules. Curr Opin Lipidol 18:121-128

Dunn TM, Lynch DL, Michaelson, LV, Napier, JA (2004) A post-genomic approach to understanding sphingolipid metabolism in Arabidopsis thaliana. Ann Bot 93:483-497

Futerman AH, Hannun YA (2004) The complex life of simple sphingolipids. EMBO reports 5:777-782

Grennan AK (2006) Genevestigator. Facilitating web-based gene-expression analysis. Plant Physiol 141:1164-1166

Guan XL, Wenk MR (2006) Mass spectrometry-based profiling of phospholipids and sphingolipids in extracts from Saccharomyces cerevisiae. Yeast 23:465-477

Hanada K, Nishijima M, Kiso M, Hasegawa A, Fujita S, Ogawa T, Akamatsu Y (1992) Sphingolipids are essential for the growth of Chinese hamster ovary cells. Restoration of the growth of a mutant defective in sphingoid base biosynthesis by exogenous sphingolipids. Journal of Biological Chemistry 267:23527-23533

Huitema K, van den Dikkenberg J, Brouwers JF, Holthuis JC (2004) Identification of a family of animal sphingomyelin synthases. EMBO J 23:33-44

Liang H, Yao N, Song JT, Luo S, Lu H, Greenberg JT (2003) Ceramides modulate programmed cell death in plants. Genes Dev 17:2636-2641

Luberto C, Stonehouse MJ, Collins EA, Marchesini N, El-Bawab S, Vasil AI, Vasil ML, Hannun YA (2003) Purification, characterization, and identification of a sphingomyelin synthase from Pseudomonas aeruginosa. PlcH is a multifunctional enzyme. J Biol Chem 278:32733-32743

Magee T, Prinen N, Alder J, Pagakis SN, Parmryd I (2002) Lipid rafts: cell surface platforms for T-cell signalling. Biol Res 35:127-131

Mina JG, Pan SY, Wansadhipathi NK, Bruce CR, Shams-Eldin H, Schwarz RT, Steel PG, Denny PW (2009) The Trypanosoma brucei sphingolipid synthase, an essential enzyme and drug target. Mol Biochem Parasitol 168:16-23

Nagiec MM, Nagiec EE, Baltisberger JA, Wells GB, Lester RL, Dickson RC (1997) Sphingolipid synthesis as a target for antifungal drugs. Complementation of the inositol phosphorylceramide synthase defect in a mutant strain of Saccharomyces cerevisiae by the AUR1 gene. J Biol Chem 272:9809-9817

Nagiec MM, Young CL, Zaworski PG, Kobayashi SD (2003) Yeast sphingolipid bypass mutants as indicators of antifungal agents selectively targeting sphingolipid synthesis. Biochem Biophys Res Commun 307:369-374

Neuwald AF (1997) An unexpected structural relationship between integral membrane phosphatases and soluble haloperoxidases. Protein Sci 6:1764-1767

Pierce SK (2002) Lipid rafts and B-cell activation. Nature Rev Immunol 2:96-105

Ralton JE, McConville MJ (1998) Delineation of three pathways of glycosylphosphatidylinositol biosynthesis in Leishmania mexicana. Precursors from different pathways are assembled on distinct pools of phosphatidylinositol and undergo fatty acid remodeling. J Biol Chem 273:4245-4257

Sato K, Noda Y, Yoda K (2009) Kei1: A novel subunit of inositolphosphorylceramide synthase, essential for its enzyme activity and Golgi localization. Mol Biol Cell 20:4444-4457

Smith WL, Merrill AH (2002) Sphingolipid metabolism and signaling. J Biol Chem 277:25841-25842

Thompson W, MacDonald G (1975) Isolation and characterization of cytidine diphosphate diglyceride from beef liver. J Biol Chem 250:6779-6785

Thompson W, MacDonald G (1976) Cytidine diphosphate diglyceride of bovine brain. Positional distribution of fatty acids and analysis of major molecular species. Eur J Biochem 65:107-111

Wang W, Yang X, Tangchaiburana S, Ndeh R, Markham JE, Tsegaye Y, Dunn TM, Wang GL, Bellizzi M, Parsons JF, Morrissey D, Bravo JE, Lynch DV, Xiao S (2008) An inositolphosphorylceramide synthase is involved in regulation of plant programmed cell death associated with defense in Arabidopsis. Plant Cell 20:3163-3179

Zhong W, Murphy DJ, Georgopapadakou NH (1999) Inhibition of yeast inositol phosphorylceramide synthase by aureobasidin A measured by a fluorometric assay. FEBS Lett 463:241-244

Table 1

EST numbers for AtIPCS genes derived from TAIR BLAST version 2.2.8.

	EST
AtIPCS1	32
AtIPCS2	57
AtIPCS3	25

Table 2

Microarray Data for AtIPCS2 in the Genevestigator database

Root	Rosette Leaf	Cauline Leaf	Stem	Flower	Siliques
2383	2135	2509	1167	998	705

Figure 1

AtIPCS1-3 complements a yeast *AUR1* auxotrophic mutant and confers aureobasidin A resistance

A. YPH499-HIS-GAL-AUR1 auxotropic yeast transformed with pRS246MET25 either empty or bearing AUR1 or AtIPCS1-3 and grown under permissive (SGR) or non-permissive conditions (SD).
B. 100μM aureobasdin A (AbA) in DMSO, 1mM myriocin (Myr) in DMSO and DMSO alone spotted in 2 and 3 μl quantities onto YPH499–HIS–GAL–AUR1 complemented with AUR1 or AtIPCS1-3 on non-permissive SD plates.

pRS426 – YPH499–HIS–GAL–AUR1 pRS426MET25; AUR - YPH499–HIS–GAL–AUR1 pRS426 ScAUR1; AtIPCS1-3 - YPH499–HIS–GAL–AUR1 pRS426 AtIPCS1-3. Grown on either permissive (non-glucose containing) SGR -HIS -URA or non-permissive (glucose containing) SD -HIS -URA.

Figure 1

A

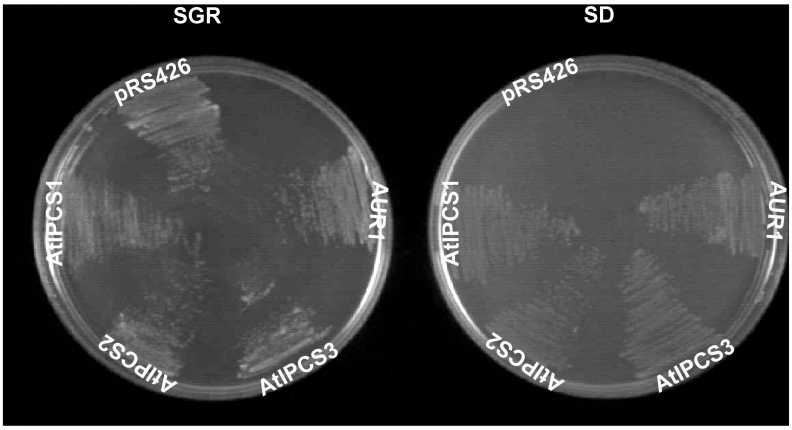
SGR
SD
pRS426
AtIPCS1
AUR1
AtIPCS2
AtIPCS3
pRS426
AtIPCS1
AUR1
AtIPCS2
AtIPCS3

B

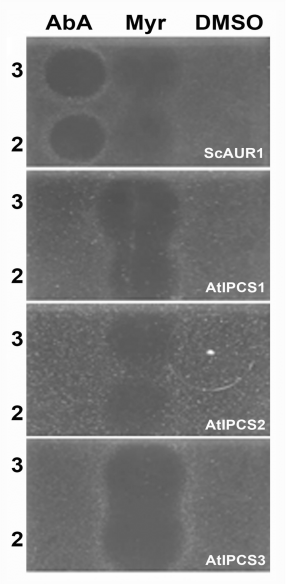
AbA
Myr
DMSO
3
2
ScAUR1
3
2
AtIPCS1
3
2
AtIPCS2
3
2
AtIPCS3

Figure 2

AtIPCS1-3 encode functional IPC synthases

In vitro assay of microsomal extracts from YPH499-HIS-GAL-AUR1 pRS246 AtIPCS1-3 and YPH499-HIS-GAL-AUR1 pRS246 AUR1.

A. Assay in the presence of phosphatidylinositol (PI) with (+) or without (-) the specific fungal inhibitor aureobasidin A (AbA). In contrast to the *S. cerevisiae* IPC synthase (AUR1), the plant activity encoded by AtIPCS1-3 is insensitive to AbA at 5 μM.
   Markers of NDB C_6-ceramide and NBD C_6-IPC, and the origin (O) indicated.

B. Assay with (+) or without (-) donor substrate PI in the presence of 5 μM AbA. Enzyme turnover is only significantly enhanced by the addition PI in the case of AtIPCS2.
   Mean of 3 separate experiments, standard error shown. A.F.U. – Arbitrary Fluorescence Units.

Figure 2

A

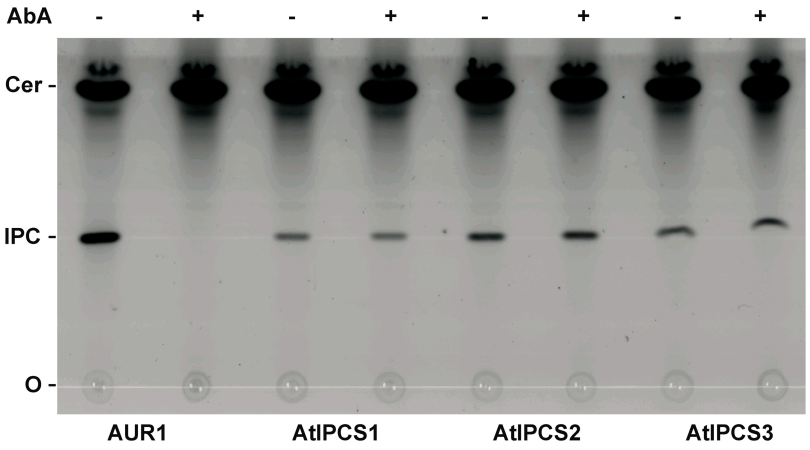
AbA - + - + - + - +
Cer
IPC
O
AUR1
AtIPCS1
AtIPCS2
AtIPCS3

B

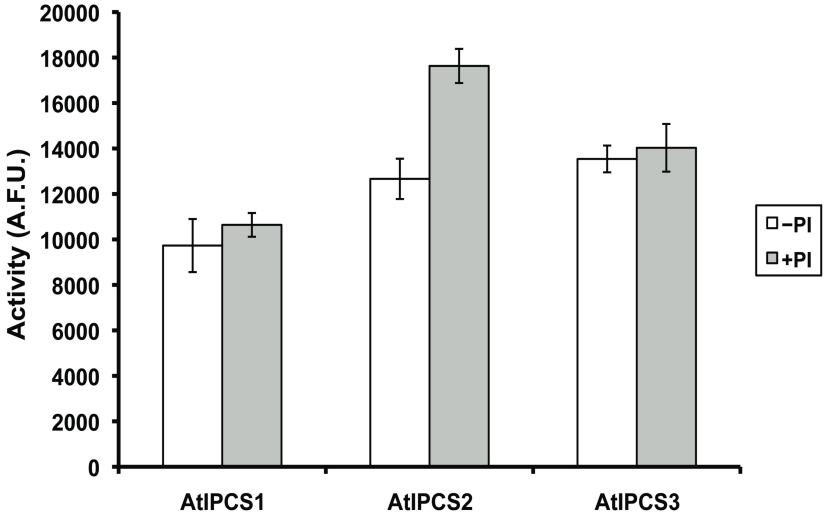
Activity (A.F.U.)
20000
18000
16000
14000
12000
10000
8000
6000
4000
2000
0
AtIPCS1
AtIPCS2
AtIPCS3
-PI
+PI

Figure 3

The plant IPC synthase defines a new class of sphingolipid synthases

Maximum parasimony analysis of Animalae, Fungi, Trypanosomatidae and Plantae sphingolipid synthase sequences. Bootstrap scores >60 indicated.

Homo sapiens LPP1 (outgroup) accession number: O14494; *Arabidopsis thaliana* IPCS1-3 accession numbers: At3g54020.1, At2g37940.1, At2g29525.1; *Oryza sativa* IPCS1-3: NP_001044812, NP_001055712, NP_001055096; *T. brucei* SLS1-4: Tb09.211.1030, Tb09.211.1020, Tb09.211.1010, Tb09.211.1000; *T. cruzi* IPCS1&2: Tc00.1047053506885.124, Tc00.1047053510729.290; *L. major* IPCS: LmjF35.4990; *Aspergillus fumigatus* AUR1p: AAD22750; *Candida albicans* AUR1p: AAB67233; *Pneumocystis carinii* AUR1p: CAH17867; *Saccharomyces cerevisiae* AUR1p: NP_012922; *Schizosaccharomyces pombe* AUR1p: Q10142; *Caenorhabditis elegans* SMS1-3: Q9U3D4, AAA82341, AAK84597; *Homo sapiens* SMS1&2: AB154421, Q8NHU3; *Mus musculus* SMS1&2: Q8VCQ6, Q9D4B1.

Figure 3

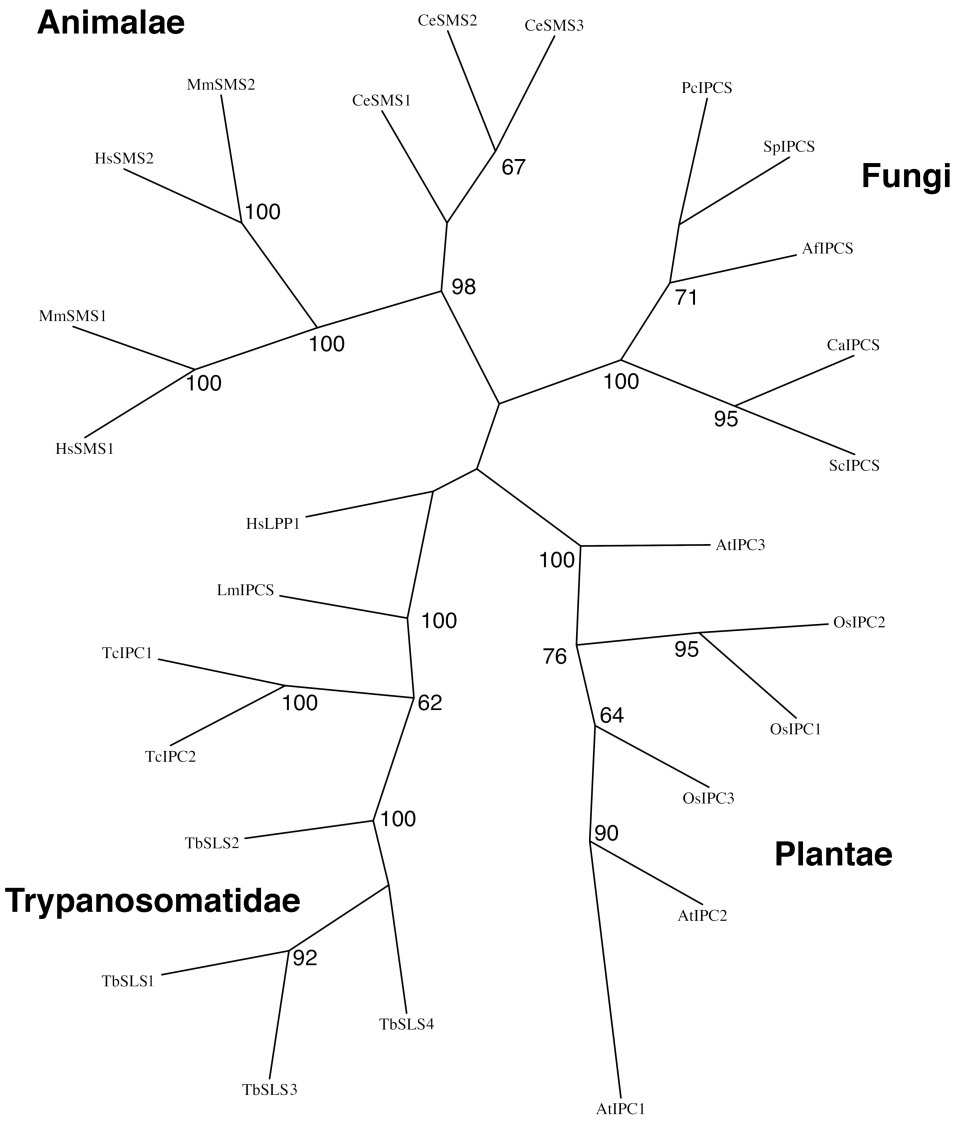
Animalae
CeSMS2
CeSMS3
MmSMS2
CeSMS1
PcIPCS
SpIPCS
HsSMS2
67
Fungi
100
AfIPCS
98
71
MmSMS1
100
CaIPCS
100
100
95
HsSMS1
ScIPCS
HsLPP1
AtIPC3
100
LmIPCS
100
OsIPC2
TcIPC1
76
95
100
62
64
OsIPC1
TcIPC2
OsIPC3
100
90
TbSLS2
Plantae
Trypanosomatidae
AtIPC2
92
TbSLS1
TbSLS4
TbSLS3
AtIPC1

Figure 4

Steady-state levels of AtIPCS isoform mRNAs in plant tissues

The numbers of AtIPCS1-3 transcripts were determined in total RNA from various tissues, by quantitative RT-PCR using a standard curve for each transcript. AtIPCS2 (At2g37940.1) is the most abundant form in roots, leaves and siliques, whereas stems and flowers have similar numbers of AtIPCS2 and AtIPCS3 (At2g29525.1) transcripts. AtIPCS1 (At3g54020.1) transcript is uniformly low in all tissues.

Figure 4

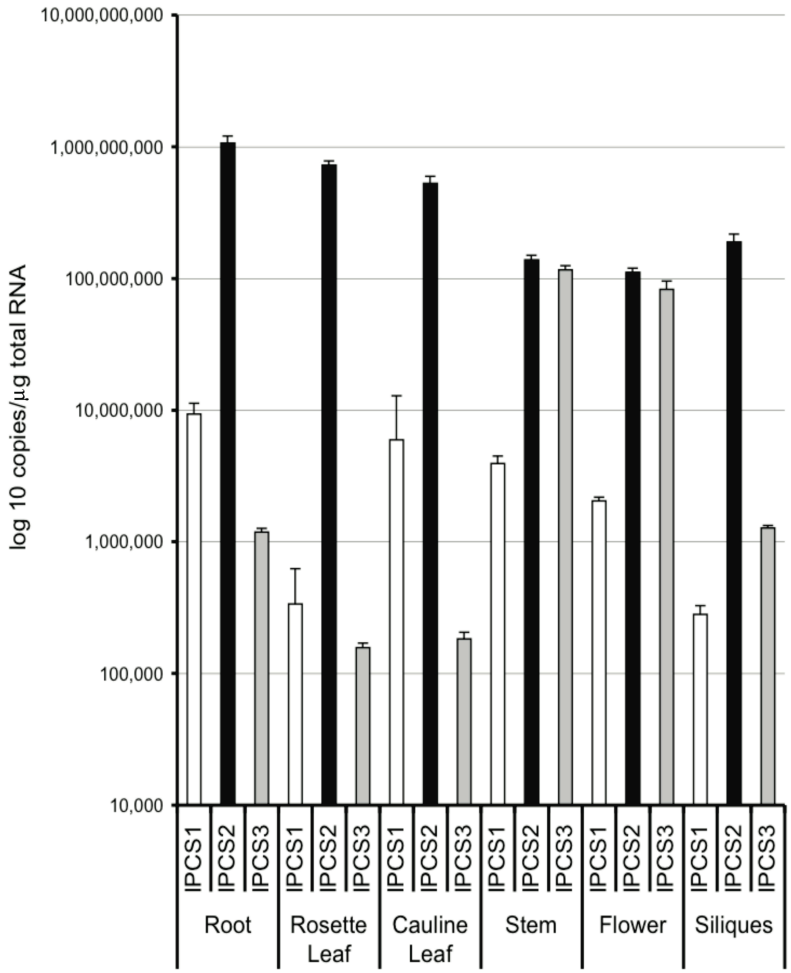
10,000,000,000
1,000,000,000
100,000,000
10,000,000
1,000,000
100,000
10,000
log 10 copies/µg total RNA
IPCS1
IPCS2
IPCS3
Root
Rosette Leaf
Cauline Leaf
Stem
Flower
Siliques